



Designing chemical micromotors that communicate-A survey of experiments

Luyang Huang^a, Jeffrey L. Moran^{b,**}, Wei Wang^{a,*}

^a School of Materials Science and Engineering, Harbin Institute of Technology (Shenzhen), 518055, Shenzhen, China

^b Department of Mechanical Engineering, George Mason University, Manassas, VA, USA



ARTICLE INFO

Keywords:

Active colloids
Micromotor
Phoresis
Interactions
Collective behaviors

ABSTRACT

Micromotors that communicate with their neighbors or with the environment are useful in a wide variety of applications, especially those involving complicated tasks that require coordination. A biomimetic strategy for achieving this goal is via chemical communication, where chemical signals released from one motor is transmitted through the medium and induce a specific response from a second motor. In this article, we review the recent experimental progress on this front. We first introduce three common strategies for releasing chemicals from a microscopic object, via diffusion, physical/chemical stimuli, or gated control, that form the cornerstone for designing communicating micromotors. We then review three levels of chemical communication of micromotors in order of ascending complexity, starting with cases where micromotors attract or repel inert tracers, to the unidirectional signal transmission between two motors of different types, and finally to the reciprocal (bidirectional) communication between two motors that often lead to higher-order assemblies. This review article ends with a perspective of the challenges and opportunities with communicating micromotors, which could inspire more sophisticated designs of in-depth communication between motors with different functions.

1. Introduction

Inspired by natural bio-motors such as myosin and kinesin [1], in the last 15 years researchers have proposed and realized the concept of “artificial micromotors”, which are synthetic microscopic particles that convert energy in the surrounding environment into autonomous motion [2–7]. Micromotors are being widely considered for applications spanning from environmental monitoring [8,9] to drug delivery [10,11], biosensing [12,13], and others. Considering their simple fabrication and high stability, micromotors have also been used as a model system for studying active matter to replace biological model systems such as cells or microorganisms.

To meet the increasingly complicated demands of practical application scenarios, micromotors need to sense changes in their environment, communicate with each other, and cooperate to accomplish complex and diverse tasks [14–17]. A possible scenario requiring such a level of sensing, communication and cooperation can be found in precision medicine therapies, especially those involving solid tumors, the micro-environment of which typically contains gradients in pH, oxygen concentration, temperature, and interstitial fluid pressure, posing challenges for the delivery of therapeutic agents. A micromotor rises to the occasion

by first sensing the spatial and temporal changes in its local environment, and responding with a change in its speed, orientation, direction, or chemical compositions. Loaded drugs can also be released. In addition, a complex environment such as that found near a tumor often requires a division of labor among different motors: for example, a first set of motors could obtain information from the external environment and relay that information to other motors that perform a necessary task. Motor-motor communication is the key to ensure correct motors receive the correct message, thus carrying out the correct actions [14]. Robust micromotor communication, both with their surroundings and with each other, would enable a spectrum of new possible strategies for delivery of therapeutic payloads. For example, if microswimmers can flocculate in response to changes in pH, they could bunch up and preferentially deliver the highest dose of medication in the most acidic regions, which is generally where the most chemotherapeutic-resistant cancer cells reside.

Using physical signals, such as sound [15], light [16], electricity [17] or magnetism [18], to activate motors' communication requires complicated signal-generating devices, which are challenging and costly to operate and may have side effects on biological tissues. In contrast, the use of chemical signals to mediate motors' communication eliminates the requirement for these devices, and the signals are retained for a longer

* Corresponding author.

** Corresponding author.

E-mail addresses: jmoran23@gmu.edu (J.L. Moran), weiwangsz@hit.edu.cn (W. Wang).

time, giving motors more time to receive and respond to information. This is often how living organisms communicate. For instance, queen bees secrete saliva and produce odors to attract worker bees to serve them [19]. Rat skeletal muscle cells proliferate and differentiate when they sense the chemokine CKLF1 [20]. *Escherichia coli* bacteria (*E. coli*) spontaneously reorient their motion using receptor proteins on their outer surface to detect a specific signal (e.g., sensing a concentration gradient), which transmit this information to the flagellar motor to alter the motion direction [21]. Over time, this leads to coordinated migration toward lower or higher concentrations, a process known as chemotaxis that is used by a wide variety of motile cells for various biological purposes. Chemotaxis allows bacteria to find nutrients or avoid predators and allows neutrophils to pursue pathogenic bacterial intruders or find sites of injury and initiate tissue repair. Thus, the secretion of chemical signals under specific scenarios is an effective means for information transfer and regulation in natural microorganisms. Inspired by these natural examples of chemical communication, micromotors capable of similar functionality are more likely to perform complex tasks in the human body and meet actual needs.

In this review article, we summarize recent advances related to chemical communication among micromotors, with an emphasis on how they respond to changes in the local chemical microenvironment and to each other's chemical signals (Fig. 1). This article is organized as follows. In section 2, we describe some common methods for locally releasing chemical stimuli: by diffusion (from porous media or gate control) or in response to a chemical or optical signal. Although the colloidal particles in these examples are not always micromotors, these studies are pertinent to the present review because the ways in which chemical signals are produced and colloidal particles (active or not) respond to such signals can serve as the foundation for designing communicating micromotors. Building upon this knowledge, in section 3 we discuss micromotor communication on three levels: 1) signals released from a micromotor and directed to inert colloids, 2) unidirectional signal transmission between two motors of different types, and 3) reciprocal (bidirectional) communication between two motors (often leading to higher-order

assemblies). Finally, in section 4, we close this article by offering our perspective of the challenges and opportunities with micromotors communicating via chemical signals.

2. Methods of releasing chemical signals

The two key components in the design of chemically communicating micromotors are 1) a chemical message that is transmitted, and 2) a mechanism for a micromotor to respond to such a message. In this section, we introduce examples of ways that small molecules or ions (such as H_2O_2 , H^+ , OH^- or F^-) can be released, and how inert particles as well as chemically active micromotors respond to these species. This response often manifests as a change in motor speeds and typically arises via diffusiophoresis or electroosmosis.

Although the focus of this article is on micromotor communication, we gain valuable information from previous studies on non-motile colloidal particles. In some examples discussed in this section, chemical signals are released via a simple mechanism (e.g., pure diffusion, as in section 2.1) which produces a chemical gradient that motors respond to. In other cases, the release mechanism is more intricate (e.g., gated or stimuli-responsive release in sections 2.2 and 2.3), but no micromotor is present (rather, the response of inert tracer particles is analyzed). The general principles introduced in section 2 lay the foundation for designing micromotors that communicate, as we see later in section 3, and for more complicated designs that remain to be developed.

2.1. Diffusion

2.1.1. General principles of diffusion

Diffusion is the simplest way to release chemicals. Diffusion is a transport process that originates from thermal motion of chemical solutes at the molecular scale. Whenever a concentration gradient of a substance is present, a net transfer of substance occurs from regions of high concentration to regions of low concentration. The steeper the gradient, the more rapidly the substance propagates. This is expressed mathematically

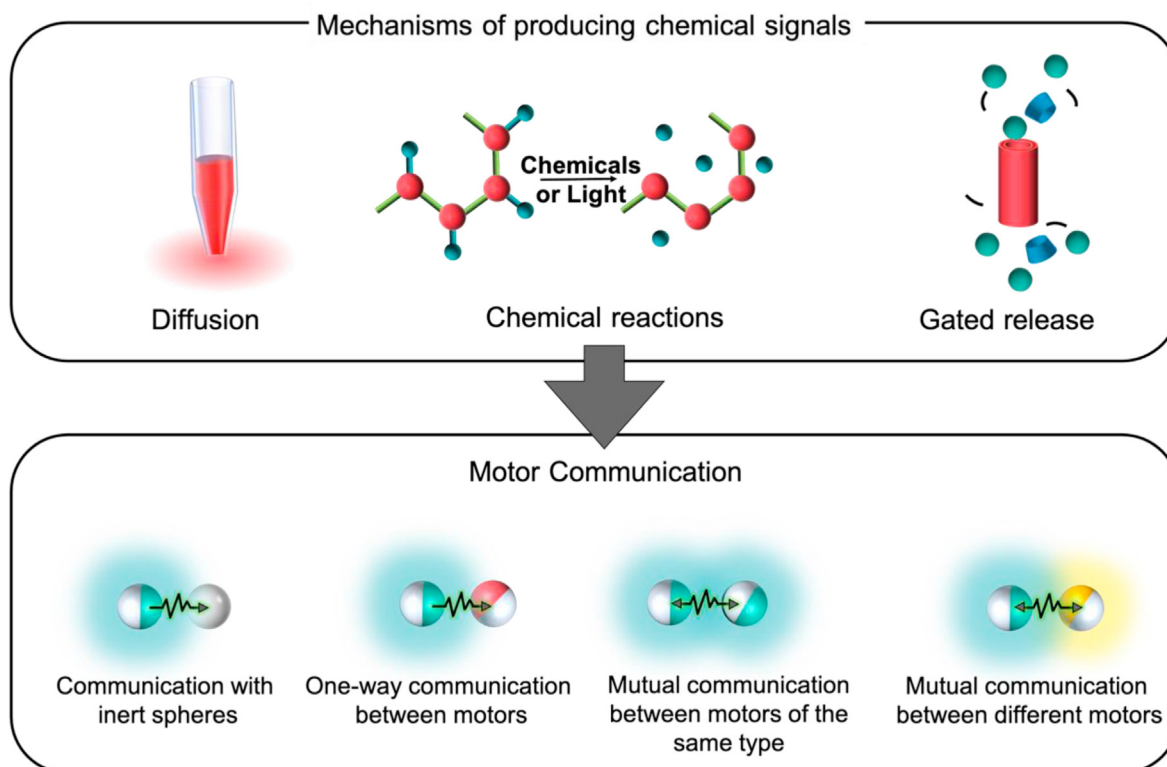


Fig. 1. A general scheme of different methods of releasing chemical signals and different types of communication exhibited by micromotors.

by Fick's First Law of Diffusion: in an ideal solution in which a substance of diffusivity D exhibits a gradient of concentration c in one direction (x), Fick's First Law is

$$J_x = -D \frac{dc}{dx},$$

where J_x is the flux in the x -direction. J_x is the amount of substance that will migrate through a unit area in the yz -plane in a unit time interval. The negative sign dictates that the flux occurs from higher to lower concentrations. Fick's Law can be easily extended to two or three dimensions, in which flux becomes a vector quantity. Once the system reaches equilibrium, the concentration is uniform everywhere, and the net flux vanishes. Since the speeds and directions of motors are often dictated by the concentrations of chemicals in their vicinity, diffusion drives the local response of many types of micromotors.

The first element of designing a system of diffusing chemicals is the choice of a carrier from which chemicals are released and by which a concentration gradient is generated and sustained. Such a carrier can take the form of a micron-sized capillary tube, a pipet tip, or a gel consisting of a three-dimensional polymer network. In the case of capillaries, the desired chemical is loaded directly into it through the capillarity force. As for gels, their porous network structure enables rapid absorption of the chemical by soaking and then filtering and washing to obtain the loaded carriers. When chemicals need to be released, the chemical-laden medium, a capillary tube or a piece of gel, can be put in contact with fresh liquid, establishing a concentration gradient that drives diffusion of the chemicals out of the gel or capillary.

2.1.2. Responding to a chemical gradient

Depending on the nature of the diffusing chemical signal, the object being studied (microorganisms, inert tracer particles, or chemically active micromotors) can respond in a variety of ways. If the subject is motile, one way is to "intentionally" alter the direction of motion up or down a concentration gradient (chemotaxis), as in the case of many microorganisms [22]. For example, Chen et al. studied the changes in sperm motility with capillaries releasing sea squirt oocyte secretion steroid (SAAF, a chemoattractant for sperms) [23], which naturally generates a concentration profile of SAAF that is higher near the capillary outlet. Note that the SAAF was apparently free to diffuse away from the capillary outlet; this may have long-term effects on chemotactic accumulation since the concentration gradient was presumably not constant in time. Sperm moved towards the capillary tip and began to move in a helical trajectory, while control experiments without SAAF saw sperms moving in circles and no directional migration toward the capillary tip. Shao et al. studied neutrophils' motility in a gradient of chemo-attractant secreted by agar-loaded *E. coli* [24]. After sensing the attractant, neutrophils were activated and moved closer to the agar. In both cases, the microorganism seeks out higher concentrations of a chemical that benefits to the organism (chemoattractant), leading to accumulation in high concentrations (positive chemotaxis). If the chemical is harmful to the organism (e.g., a poison or chemical secreted by a predator), microorganisms such as *E. coli* can reorient their motion toward lower concentrations (negative chemotaxis).

Although it can co-occur with chemotaxis, chemokinesis is a separate phenomenon whereby an organism's speed is increased or decreased as the concentration of a chemical is changed. If the chemical is not a chemotactic factor, cells undergoing chemokinesis change their speed *without* changing their direction in response to changes in chemokine concentration. Wilkinson et al. studied a system in which human neutrophils swam above a glass surface divided into two regions, one coated with the protein bovine serum albumin (BSA) and one coated with anti-BSA Immunoglobulin G (IgG) antibodies; the speeds of the cells were higher on BSA than on anti-BSA, but their reorientation frequency was unchanged on the two substrates [25]. Over time, the neutrophils preferentially accumulated in the anti-BSA-coated regions (where their

motility was minimized), suggesting that the accumulation arose from the organisms' chemokinesis and their random turning events, and that chemotaxis is not necessary to cause cell accumulation in a chemical gradient. The difference between chemotaxis and chemokinesis is further elaborated in section 2.1.3.

Inspired by natural chemotaxis, Hong et al. demonstrated that synthetic microswimmers, i.e. bimetallic (gold-platinum) microrods, accumulate in regions that are initially rich in H_2O_2 [26]. The gel was soaked with 30 wt% H_2O_2 in advance and then placed in the solution, slowly releasing H_2O_2 by diffusion. Thereafter, the Pt/Au rods sensed H_2O_2 and gathered near the gel. As shown in Fig. 2a, as time passed more rods gathered in the gel's vicinity while simultaneously more H_2O_2 was released. These observations are surprising and not without controversy, given that synthetic microswimmers lack the intricate biological mechanisms that enable them to "remember" the local concentration and make turns when needed. Furthermore, the presumed chemoattractant in these experiments (H_2O_2) was free to diffuse, meaning the concentration gradient was not constant in time and may have dissipated by the time the accumulation was observed. More recently, when placed in an H_2O_2 gradient that was maintained constant in time, Pt/Au rods were observed to accumulate in the *lowest* H_2O_2 concentration regions by chemokinesis [27], a similar result to those observed previously with neutrophils from Wilkinson et al. [25].

In addition to fuel, micromotors can also exhibit a speed dependence on pH (what could be called "pH-kinesis"), and thus a pH gradient can lead to macroscopic, directional transport of microparticles. For example, Bhuyan et al. investigated the motion of mushroom debris, whose surface contains catalase, in gradients of NaOH and HCl [28]. Because the rate of catalytic decomposition of H_2O_2 by catalase strongly depends on pH, these mushroom debris are found to move towards regions of high pH. Similarly, Dey et al. found that polymer microspheres decorated with palladium nanoparticles moved toward regions of high pH (Fig. 2b) [29]. In both experiments, chemicals are released from a reservoir via a cotton thread that connects it to the solution. Recently, Archer et al. demonstrated that micromotors fabricated from a cationic hydrogel, poly(2-vinyl pyridine), swell as the pH is decreased (therefore slowing the micromotor), causing them to accumulate in the most acidic regions and preferentially release their onboard cargo in these same regions [30]. This work has potential application to cancer treatment, since cancer cells are widely known to create a locally acidic environment, leading to a pH gradient that may be exploited for payload delivery [31].

Another mechanism for a colloidal object to react to a chemical signal is by altering the interfacial tension distribution in its vicinity and "surfing" with the resulting Marangoni flow. For example, Lagzi et al. designed an experiment in which an oil droplet moves in this manner and rapidly solves a maze via pH-taxis [32]. The maze was filled with a KOH solution and agar loaded with HCl (pH 1.2) was placed at one of the maze inlets, where HCl was released by diffusion and a concentration gradient was generated throughout the maze (Fig. 2c). A droplet of a mixture of dichloromethane and hexadecanoic acid entered the labyrinth and encountered a gradient of pH between its front and back. Because hexadecanoic acid is easily protonated at the side of the droplet where pH is low, its surface tension is reduced, while the surface tension is higher on the other end of the droplet. A gradient of surface tension therefore propels the droplet toward the exit where the pH (and therefore the surface tension) is the lowest, thereby solving the maze.

Inspired by the work of Lagzi et al., Jin et al. demonstrated that chemotactic oil droplets in a surfactant solution undergo chemotaxis in a surfactant gradient [34]. The droplets were constituted from a nematic liquid crystal and the ionic surfactant used was tetradecyltrimethylammonium bromide (TTAB). The propulsion is governed by Marangoni flows established by gradients in interfacial tension along the droplet. As oil dissolved in the surfactant solution, oil molecules migrated into the surfactant micelles. As this happens, filled micelles disperse from the droplet into the solution. When the droplet moves, it encounters more empty micelles in the front and leaves more oil-filled micelles behind.

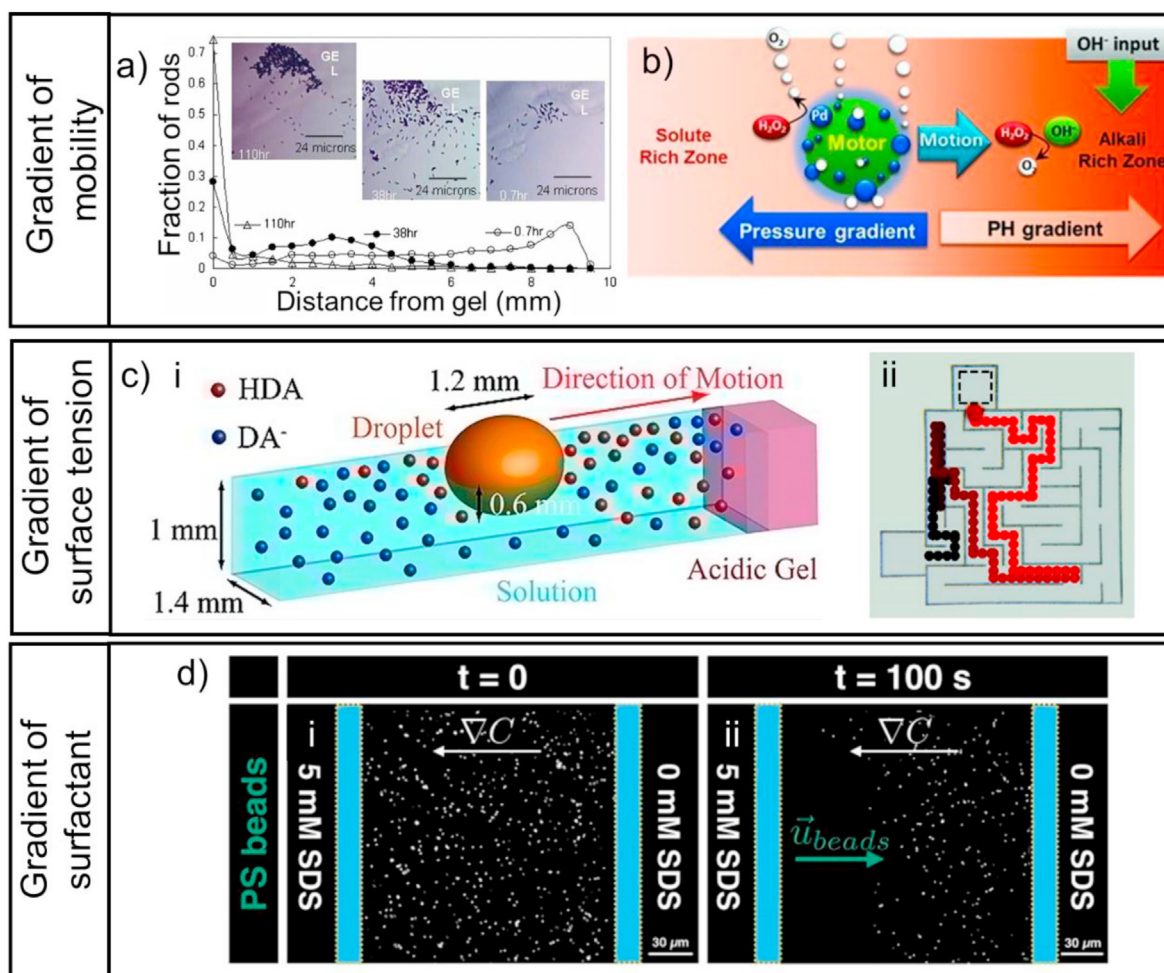


Fig. 2. Release of chemicals via diffusion can cause gradients of mobility (a, b), surface tension (c) or surfactant (d). a) Distribution of Pt/Au rods in a H_2O_2 concentration gradient released by gel at 0.7 h, 38 h, and 110 h [26]. b) NaOH is released from a cotton thread connected to a reservoir. Because of the different pH values at the two sides of the microspheres, the catalytic decomposition of H_2O_2 is faster on the right side than on the left, causing it to move from left to right [29]. c) A droplet moves in a gradient of acid (i) and solves a maze (ii) [32]. d) Polystyrene tracers that are initially distributed uniformly ($t = 0$) migrate diffusio-phoretically down a concentration gradient of the surfactant sodium dodecyl sulfate (SDS) [33].

This micelle gradient establishes an inhomogeneous coverage of surfactant on the surface of the droplet, establishing a gradient in interfacial tension that drives Marangoni flows. The net migration is toward higher surfactant concentration. As in the work of Lagzi et al., the droplets demonstrated chemotaxis by successfully solving a microfluidic maze in which a TTAB source was placed at the exit.

The above examples demonstrate that while chemotaxis is usually carried out in microorganisms via sensing and signaling at the single-cell level, chemotaxis-like behaviors can be realized in nonliving systems in a rich variety of ways that are distinct from the biological mechanisms for chemotaxis [35].

A third mechanism of micromotors responding to a chemical gradient is via electrokinetics. In particular, the diffusion of ions of different diffusivities generates a diffusion potential and an associated electric field that retards the fast-diffusing ions and accelerates the slow-diffusing ones. If the particle is charged, this electric field can then induce motion by electrophoresis (though, since the origin of the field is the concentration gradient, it is considered a component of diffusiophoresis) [36]. A charged particle exposed to this electric field could undergo electrophoresis (specifically the electrophoretic component of ionic diffusiophoresis) [37], or be dragged by the electroosmotic flow occurring on a charged substrate [38]. To showcase this principle, Banerjee and Squires demonstrated the “solutoinertial phenomenon” whereby immobilized structures or suspended particles release solute into solution

and attract or repel other colloidal particles in suspension. The particle transport mechanism in this case is a combination of diffusiophoresis (arising from the gradient of SDS, the released solute) and possibly Marangoni effects (arising from the gradient in interfacial tension arising from the gradient in SDS). As shown in Fig. 2d, in one example, a piece of polyethylene glycol diacrylate (PEGDA) gel releases sodium dodecyl sulfate (SDS) [33], which dissociates into sodium cations (Na^+) and an accompanying anion; the Na^+ diffuses much faster than the anion, and this asymmetry establishes an electric field towards the gel “beacon” that repels negatively charged polystyrene tracer spheres. Although only inert particles are used in this experiment, we shall see in section 3 that these types of electrokinetic interactions are commonly used to engineer micromotors that communicate.

The above examples show that releasing chemical substances by diffusion is simple and easy to operate. Choosing the appropriate chemical makes it possible to induce motors to accelerate, change the mode of motion, and solve mazes at micro- and nanoscales. Therefore, it can be used as a model system to study the dynamics of micromotors in a changing chemical microenvironment. However, in a strictly diffusion-dominated system, it is difficult to control the amount of chemical released or the rate at which it spreads. Besides, to prevent the system from rapidly reaching chemical equilibrium, the carrier needs to be loaded with a large amount of chemicals at high concentrations to produce a long-lasting concentration gradient, possibly resulting in

convection that could obstruct the observation of micromotors. These disadvantages can be mitigated with better designs of controlled release of chemicals, whether preloaded or generated in situ, a topic we discuss in the next two subsections.

2.1.3. Chemotaxis vs chemokinesis

As we described above, an active particle can respond to a chemical gradient via either chemotaxis or chemokinesis. These two processes of similar names but distinct natures deserve further clarification here. Chemotaxis occurs when the *direction* of an organism or micromotor's motion is determined by the non-uniform distribution of a chemical; it thus implies a vector quantity [39,40]. Chemokinesis occurs when the *speed* (translational or rotational) of a cell or micromotor depends on the local chemical concentration and thus implies a scalar quantity [40]. Chemotaxis and chemokinesis are not mutually exclusive and can sometimes co-occur in the same organism [41,42]. However, it is important to carefully distinguish the two since they can both lead to accumulation of cells or micromotors in certain regions and are sometimes confused for each other [43,44].

For some artificial microswimmers, such as the well-studied platinum/gold (Pt/Au) hydrogen-peroxide-powered self-propelled rods, chemokinesis is immediately evident (speed increases with H_2O_2 concentration) but the occurrence of chemotaxis is less established. Recently, Moran et al. demonstrated that in a steady-state concentration gradient of H_2O_2 , Pt/Au rods accumulate over time in the regions where H_2O_2 concentration (and, therefore, their speed) is minimized, which is the opposite of what one would expect from positive chemotaxis. The authors showed that the accumulation could be quantitatively predicted by modeling the situation as a random diffusion process with a spatially-dependent diffusivity (since, because of chemokinesis, a gradient in fuel concentration implies a variation of effective diffusivity with space). This work corroborates earlier studies that found that if the turning frequency of a microswimmer is unaffected by fuel concentration, at long times microswimmers tended to dwell in low-mobility regions [22]. Thus, the accumulation could be explained not by invoking chemotaxis, but rather by identifying the coupling of chemokinesis and the random reorientation events driven by rotational Brownian motion.

The conditions in which two-faced "Janus" microswimmers, such as the Pt/Au rods, demonstrate chemokinesis and chemotaxis were theoretically analyzed by Popescu et al. [45]. The key property that dictates a microswimmer's chemokinetic or chemotactic response is the phoretic mobility, which quantifies the force exerted on the particle by a gradient of a given magnitude [46]. For example, in the case of self-electrophoresis, in which the particle propels itself due to a self-generated electric field, phoretic mobility is proportional to surface charge. The main conclusion of the analysis by Popescu et al. was that the *chemotactic* response of a Janus particle is dictated by the *difference* in phoretic mobility from its forward-facing to its backward-facing half, while the *chemokinetic* response is dictated by the surface-average of the phoretic mobility. Thus, if a Janus particle exhibits both a significant difference in mobility from front to back and a nonzero area-average phoretic mobility, the particle could exhibit both chemotaxis and chemokinesis. The sign of the difference in mobility would determine whether the chemotaxis was positive or negative.

Other designs of artificial microswimmers have demonstrated evidence of chemotactic behavior, such as newly-developed micromotors that use enzymes as engines to convert chemical energy from the enzyme's substrate into motion. For example, artificial liposomes coated with urease, catalase, and/or ATPase enzymes were found to exhibit positive or negative chemotaxis depending on the enzyme [47]. Another study demonstrated that synthetic vesicles incorporating glucose oxidase and catalase enzymes propel themselves using glucose as a fuel and demonstrated chemotaxis in glucose gradients [48]. Intriguingly, they also demonstrated evidence of blood-brain barrier crossing in mouse models, a key step in many therapeutic applications. Because of the biocompatibility of enzymes and their chemotactic capabilities,

enzymatic micromotors are expected to find wide application in biomedical settings.

2.2. Externally cued chemical signals

In addition to releasing chemicals that are pre-loaded, chemicals can also be produced in situ by external stimuli, e.g., by adding other chemicals that trigger a reaction, or by applying light. In the first case, once the excitation is applied, the reaction starts, and the release of the product will continue as long as the reaction persists. In the second case, by injecting energy through the appropriate wavelength of light, the chemical bonds of the reactants are broken to produce free radicals, and the free radicals are coupled to produce new chemicals. In this case, the chemical signal ceases as soon as the light is switched off, endowing the system with on-off switchability. These two mechanisms of stimulus-responsive release of chemical signals are introduced in this section.

A typical example of reaction-generated chemical signals is the depolymerization of long polymer chains into monomers by the addition of an initiator. For example, Zhang et al. demonstrated that a tert-butyltrimethylsilyl block-terminated poly(phthalaldehyde-based) (TBS-PPHA) film depolymerizes in the presence of F^- [49], releasing monomer molecules that accumulate near the film. As a result of the increased osmotic pressure, fluid flows toward the membrane from the sides and up at the center of the film, with the film effectively operating as a fluid pump. The scheme is shown in Fig. 3a. The release of chemical signals can be made autocatalytic, as shown by Baker et al. [50], by taking advantage of the released F^- that reacted with the functional groups on a polymer microsphere that released more F^- as shown in Fig. 3b. As a result, once initiated (by light in this case), the reaction continues and self-amplifies, causing a strong pumping effect of nearby fluids. Although this example pertains to chemical micropumps, its operating principle can be easily implemented in a micromotor design.

While the above examples require specific initiator excitation to release new chemicals, incident light can also trigger reactions that release chemicals. This method is controllable, and the substance release stops when turning off the stimulus (i.e., the light source). For example, Yadav et al. designed an ultraviolet light (UV)-driven pump with an on/off switch by activating a photoacid initiator with light of proper wavelength in Fig. 3c [51]. The photoacid initiator N-hydroxyphthalimide triflate dissociates into CF_3SO_3^- and H^+ when illuminated by 365 nm light. Because the anion and cation diffused at different rates, an electric field was generated and pulls positively charged tracer microspheres toward the photoacid initiator at a speed of $7.2 \pm 2.4 \mu\text{m/s}$. Similarly, light-induced water splitting by TiO_2 can be used to controllably release chemicals. For example, Hong et al. [52] showed that when a collection of SiO_2 and TiO_2 microspheres was irradiated with UV light (wavelength 365 nm), the photocatalytic TiO_2 microparticles generated $\cdot\text{O}_2^-$, $\cdot\text{OH}$, H^+ and OH^- , the diffusion of which generated a diffusion potential and an associated electric field that expelled charged SiO_2 microspheres from TiO_2 particles. By switching the light on and off, TiO_2 particles and SiO_2 particles can cluster together or burst apart, forming a reversible "firework." UV light can also be the fuel source for certain micromotor designs, leveraging the photocatalytic properties of anatase TiO_2 , and these also release chemicals into the surrounding fluid as they move [53].

All the systems considered in this subsection produce new chemicals in response to a specific stimulus, which induces a directional movement of the surrounding fluid, tracers, or themselves. Releasing chemicals under external stimuli alleviates the disadvantages of releasing chemical signals via simple diffusion (section 2.1) that cannot be released at a controlled rate and is thus more conducive to the design of communicating micromotors. However, using chemical reactions to release chemical signals may bring a hidden danger since it will often produce by-products such as polymers, salt ions, and organic solvents which may disrupt the system. It also means that motors will receive multiple signals at once, potentially disrupting or confusing their programmed performance. Also, the inability to know precisely which substance is operative

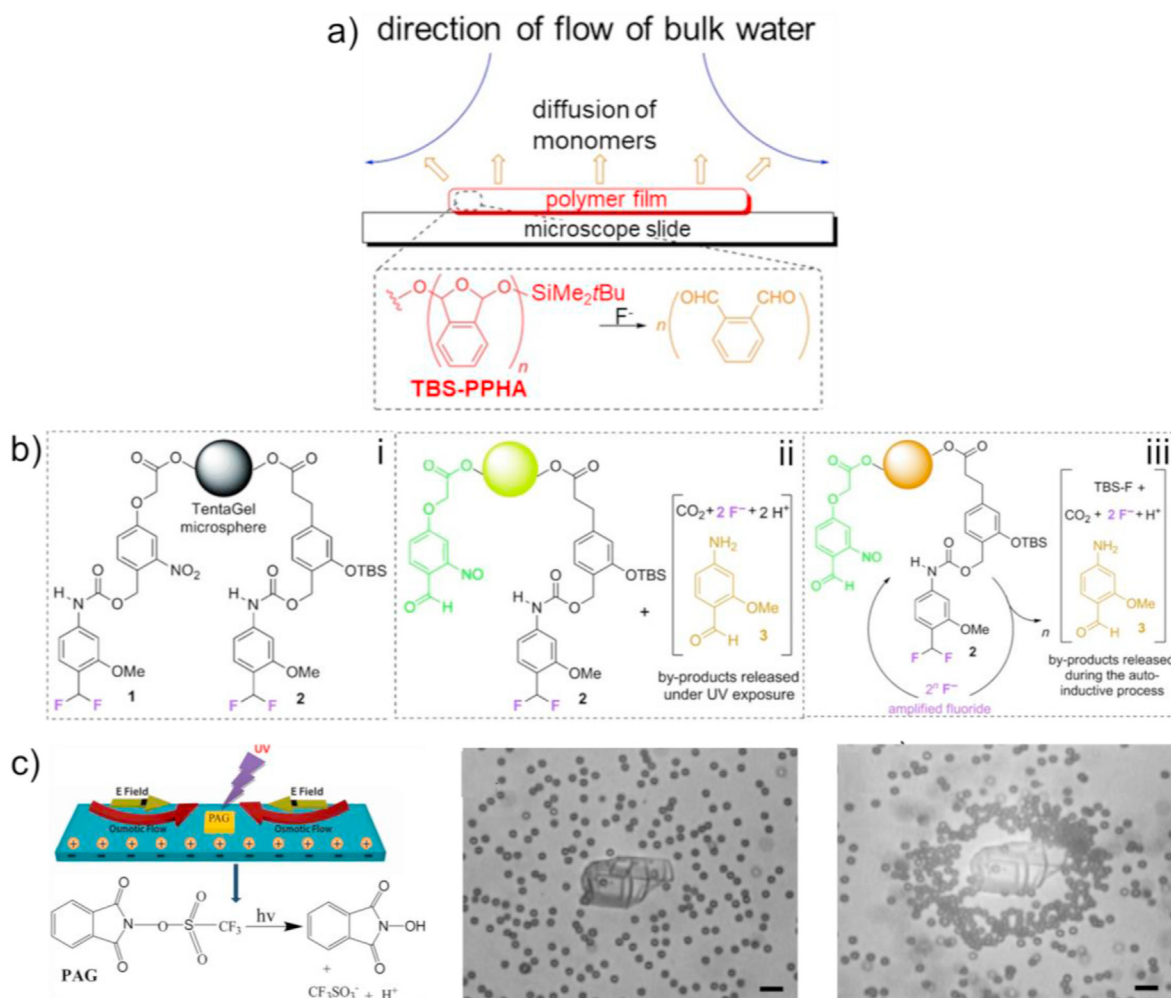


Fig. 3. Generating chemical signals under external stimuli. a) When exposed to F^- ions, a piece of polymer (TBS-PPHA) film depolymerizes and releases monomer molecules, leading to a self-powered micropump [49]. b) UV illumination initiates a self-propagating reaction that generates fluoride ions [50]. c) Under UV, polymer PAG dissociates into protons that induce electroosmotic pumping of nearby tracer particles [51].

for a given situation will make systematic and quantitative study difficult. Future research should address these challenges. Researchers need to carefully consider the byproducts micromotors generate and assess the harm they cause to sensitive system components. For example, if the intended application is water remediation, it would be unwise to use micromotors that generate toxic byproducts as a result of their motion.

2.3. “Gate control” for controlled release of loaded chemicals

The last controlled release method is to encapsulate chemicals in a carrier with a switching system in advance and release chemicals by applying a stimulus such as a change in temperature or pH, light of a specific wavelength, or a reducing agent to open the gates and control the release of the chemical. Compared with the diffusion release method, this “gate control” method can reduce the chance of premature release and enable precise timing of the release, which is important for applications such as drug delivery. Also, the “gate-controlled” carriers can be prepared at the micro/nanometer level, which is unlikely to cause convective flows that would interfere with motors’ motion. More importantly, the carrier can be loaded with a wide variety of chemicals. This contrasts with §2.2, where the chemicals released only derive from the reactants. A gate-controlled carrier can be a stimulus-responsive hydrogel, which is gated by azobenzene that responds to light. Alternatively, iron (III) oxide (Fe_2O_3) spheres or metal nanoparticles can be connected to surface of mesoporous silica microspheres using disulfide bonds to act as a “gate”.

There are also a few systems that directly connect drug molecules to a carrier with the help of a “door lock” mechanism, which breaks to release the loaded chemicals.

In 2019, Banerjee et al. improved on the soluto-inertial work described in Section 2.1 by releasing chemicals with temperature-sensitive hydrogels and investigated the collective migration of a large number of inert spheres in response to a substance gradient [54]. As shown in Fig. 4a, the beacon consisted of a temperature-sensitive polymer, poly(N-isopropylacrylamide) (PNIPAM), and internally loaded α -ketoglutarate. Above the Lower Critical Solution Temperature (LCST), PNIPAM attains a hydrophobic contraction state, where solutes are trapped in PNIPAM. Below the LCST, however, PNIPAM becomes hydrophilic and swells, opening its pores, so solutes can be released from the gap. Therefore, PNIPAM can be used as a carrier for the controlled release of chemicals. Because of the difference in the diffusion speed of H^+ and anions produced by α -ketoglutaric acid, a local electric field was generated towards PNIPAM. The negatively charged PS sphere therefore moved away from PNIPAM gel, mimicking how prey animals escape from predators.

Since the structure of PNIPAM is a three-dimensional network, the problem of pre-release of loaded chemicals leaking from the network structure is unavoidable. To address this problem, You et al. prepared a controlled release carrier with a gated structure by grafting PNIPAM onto the surface of mesoporous silica with disulfide bonds (the PNIPAM covering the pores serves as the “gate” for the controlled release of

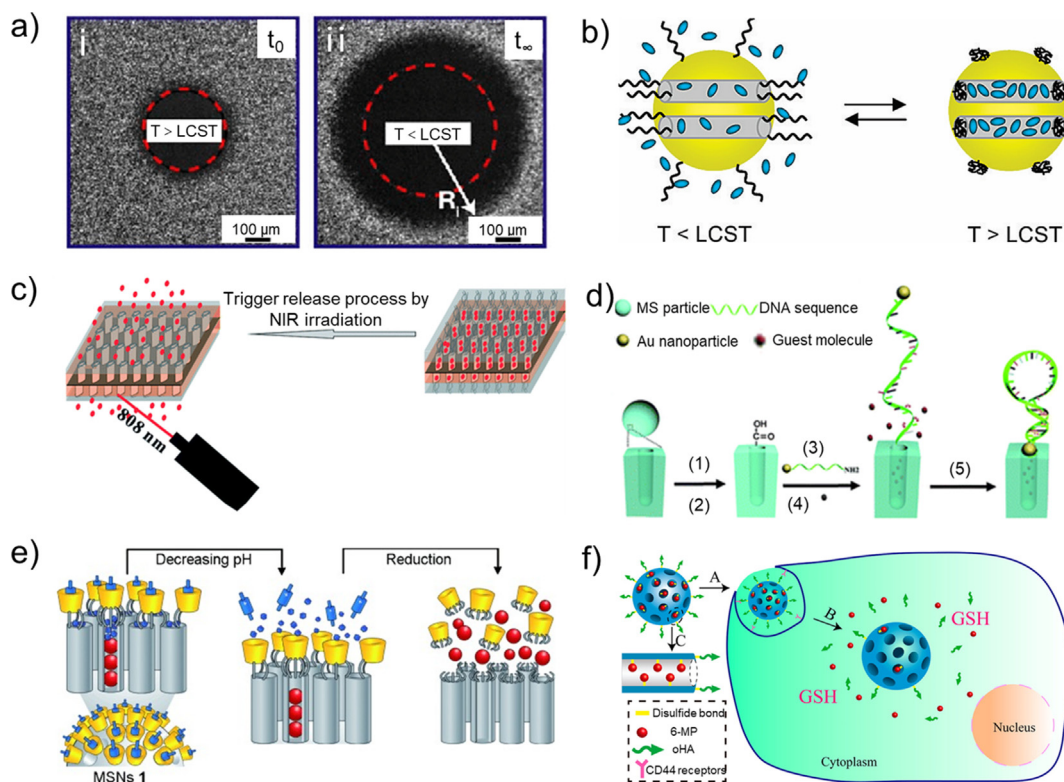


Fig. 4. Controlled release of loaded chemicals via “gate control”. a) A temperature increase triggered a phase change in a piece of PNIPAM gel, which releases solute molecules that caused tracer particles to move away from the gel and formed an exclusion zone [54]. b) PNIPAM chains stretch at $T < LCST$, and the gate opens, releasing the chemicals [55]. c) The heat generated by nanographene oxide layer makes the PNIPAM chain stretch, and release chemicals from mesoporous silica [57]. d) The reversible “opening” and “closing” of the pores can be realized by controlled assembly of AuNPs, which allowed the entrapped molecules to be retained or escape from the carrier [59]. e) Schematic representation of the dual-cargo release process. Dual cargos can be released one at a time by first lowering the pH and then adding mercaptoethanol [60]. f) Chemicals are released by breaking the disulfide bond when a reducing agent is added [62].

chemicals) [55]. Fig. 4b shows the carrier’s structure and release principle. Below the LCST, the PNIPAM chains stretched and the gates opened to release chemicals. When the temperature was raised above the LCST, the PNIPAM chains shrank and the gates were closed to terminate the release of chemicals. Note that the switching between hydrophilic and hydrophobic states, via the controlled swelling and collapse of PNIPAM under different temperatures, has been cleverly implemented on a Au–Pt micromotor to switch its propulsion between self-electrophoresis and self-diffusiophoresis [56]. However, we do not go into details because there is no chemical released in this example. In principle, these thermoresponsive PNIPAM polymer brushes could act as “gate control” mechanisms in future demonstrations in which a chemical payload stored onboard the micromotor is released on command (e.g., by locally heating the PNIPAM above the LCST); however, such an approach could have unintended consequences, as we discuss below.

The above example requires the controlled release of chemicals by varying temperature, which is not applicable for biological tissues that are heat-sensitive. Besides, heat is not a stimulus that can be simply manipulated. Not only does it require the heating platform to be in contact with the heated object, it also cannot produce an instantaneous response because it takes a finite period to heat to a response temperature. To address this problem, Wan et al. prepared a structure based on the above system for controlled release by light [57]. As shown in Fig. 4c, a nanographene oxide layer was chemically prepared on a mesoporous silica surface. Then, thermoresponsive polymer brushes were grafted onto SiO₂ through atom transfer radical polymerization. The graphene oxide nanolayer rapidly converts near-infrared light into heat, and the loaded drug can be released by opening the heat-responsive polymer valve outside the SiO₂ pore. Finally, we would like to note that heating, applied directly or via the photothermal effect, introduces changes

beyond temperature-induced chemical release described above. Notable side effects include a change in the viscosity of the medium, additional particle migration mechanisms (such as the Soret effect) arising from suddenly-imposed temperature gradients [58], or in the magnitude of diffusion of both the chemicals released and microscopic objects of interest, and these changes must be taken into consideration when designing micromotors that respond to temperature-induced chemical signals.

In addition to temperature-sensitive hydrogels, some nanoparticles can also be used as “gates” that are triggered by light. Wen et al. demonstrated a wavelength-modulated system for triggering the controlled release of chemical substances based on mesoporous silica [59]. The system was capped with Au nanoparticles modified with single-stranded DNA containing azobenzene groups as Fig. 4d shown. Single strands of DNA reacted with carboxylic acid groups generated on the surface of mesoporous silica. Under 450 nm light, the azobenzene molecule existed in a trans conformation, the single-stranded DNA formed a hairpin structure, and the Au nanoparticles clogged the pores so that the drug cannot be released. However, when the system was irradiated with 365 nm UV light, the azobenzene conformation changed to cis, the hairpin structure was unstable, the DNA unfolded in single-stranded form, and the drug molecule could be released. The fluorescence intensity changed cyclically under UV and visible light irradiation, and the drug release system was highly reversible.

In addition to using some metal nanoparticles as a “gate”, cyclodextrin with a conical stereoscopic ring structure can play the same role. Wang et al. used cyclodextrin, methyl orange, and mesoporous silica to prepare a system that can achieve controlled release based on size selection [60]. The selective release process of chemicals with different sizes is shown in Fig. 4e. The large molecule drug Hoechst 33342 was

loaded into the mesoporous silica beforehand, and then the cyclodextrin was connected to the cavity through a disulfide bond to prevent the release of the large molecule drug. At the same time, another small molecule drug, coumaric acid, could enter the mesoporous silica through the cavity in the middle of the cyclodextrin, and then the pH-responsive methyl orange was used as a gate plug to block the cavity in the middle of the cyclodextrin. Neither drug molecule can be released at this time. When the pH value was lowered, methyl orange was protonated, separating from the cyclodextrin and allowing the release of small molecules. With the addition of the disulfide bond reducing agent mercaptoethanol, the disulfide bond between cyclodextrin and mesoporous silica broke, and the macromolecule drug was released. A similar releasing mechanism via breaking disulfide bonds has been implemented in a mesoporous SiO₂ nanomotor to release drug molecules [61].

In addition to sealing the chemicals in the carrier with the aid of a gating system, the drug molecule can also be directly connected to the carrier with the aid of a “door lock.” For example, Wang et al. simplified the gating system by connecting the chemicals directly to the carrier through disulfide bonds, which can be cleaved directly when the chemicals need to be released [62]. As shown in Fig. 4f, they used thiol-functionalized mesoporous silica beads as carriers and combined the sulfhydryl-containing drug 6-mercaptopurine with the carriers through a cleavable disulfide bond. In the presence of glutathione, the disulfide bond broke, and the drug molecule could be released. The cumulative release of 6-mercaptopurine was less than 3% in the absence of glutathione and approximately 80% in 2 h in the presence of 3 mM glutathione, demonstrating the feasibility of this controlled release approach.

The above methods of using temperature-sensitive hydrogels, modifying PNIPAM on the surface of mesoporous silica, or plugging the holes of mesoporous silica beads, can control the release of chemicals by applying the appropriate stimulus to release the desired chemicals and cut off the stimulus when not needed. However, these systems are generally small, mostly in the nanometer range, with a few in the micron range, and therefore do not carry much chemical load. When the motor's sensitivity is low, in other words, triggering the motor requires a higher concentration of chemicals. If the trigger is not sufficient, “signal amplification” should be considered. If the release of chemicals is added by increasing the number of carriers, a higher dose of initiator is needed, which leads to the problem of accumulation of carrier shells in a biologically relevant environment. The threshold of initiator that the organism can tolerate, and that of metabolism of the carrier shells, should also be considered.

Chemically driven micro- and nanomotors, whether they are self-electrophoretic, self-diffusiophoretic or bubble-propelled, generally require the presence of specific fuel molecules, which are inevitably associated with small-molecule fuels such as H₂O₂, H⁺ and OH⁻. In practical applications, such as sensing, targeted drug release, environmental sensing and so on, it is often necessary for the motor to sense local specific chemical substances to produce start-stop, acceleration [63], deceleration, and other behaviors. However, these gating systems are mostly utilized to release chemical substances with large molecular weight at present, and there is little research on small-molecule chemicals. Although these gating systems cannot be used directly in motor research, they can provide some models for the design of controlled release chemical signals.

3. Communication between micromotors and (motile or non-motile) particles via chemical signals

Communication among micromotors and between micromotors and non-motile particles will be a crucial component of the design of future micromotor systems that exhibit sophisticated collective behaviors. Previous studies have shown that micro- and nanomotors have the potential to release chemicals such as H⁺ and O₂ from Au–Pt bimetallic rods, PS–Pt and TiO₂–SiO₂ Janus motors; H⁺ and Cl⁻ from AgCl motors;

and H⁺, Cl⁻ and Ag⁺ from motors containing silver. These capabilities provide the theoretical basis for chemical communication between motors. In this section, we describe chemical communication between micromotors and other objects at three levels. The first level is how released chemicals from a micromotor collect, disperse, and transport nearby inert particles. The second level is how the released chemicals from a micromotor unilaterally affect the motion of other types of motors that cannot release chemical signals. The third level discusses how motors that can release chemical signals bilaterally affect each other.

3.1. Chemical communication between motor and inert particles

Communication between micromotors and inert particles is unidirectional, with the motor acting as the sender of the message. As discussed in section 2, motors typically start transmitting a chemical message to the outside world after a specific external stimulus is applied. Upon receiving the message, inert particles can respond by moving. The response mechanism is often based on a local electric field generated by an asymmetric chemical reaction on the surface of motors, which leads to an electrophoretic force on the charged inert spheres or drives them for directional movement by the electroosmotic flow near the charged substrate.

Wang et al. investigated the collection of inert spheres by a Pt/Au bimetallic micromotor based on the release of chemicals from bimetallic rods [64]. The redox reactions on the Pt and Au surfaces resulted in the generation of H⁺ at the Pt end and consumption of H⁺ at the Au end, resulting in an electric field directed from the Pt end to the Au end. This electric field exerts a propulsive force on the negatively charged rod, leading to motion by self-electrophoresis [65–67]. The interactions between inert spheres and bimetallic rods are shown in Fig. 5a. When positively charged tracers (aminated PS spheres) were added, they preferentially gathered in the fluid region close to the Au, which carries a negative charge compared to Pt. Conversely, negatively charged tracers (PS or gold spheres) gathered near the Pt side, where the fluid is positively charged due to the buildup of H⁺ ions from the surface reactions [67]. Bimetallic rods collected up to eight densely stacked inert spheres at one end, eventually forming a stable two-dimensional raft-like structure.

Gao et al. achieved reversible assembly and dissociation of SiO₂ tracers in situ based on self-electrophoretic TiO₂/Pt motors, as shown in Fig. 5b [68]. The propulsion mechanism is essentially the same as the Pt/Au rods, in that the TiO₂/Pt motors inject and consume protons on the forward-facing (TiO₂) and backward-facing (Pt) faces respectively; in the case of TiO₂/Pt motors, the charge transfer reactions do not result from catalytic decomposition of H₂O₂ but from electron-hole separation that occurs in TiO₂ in the presence of UV. As in the work of Wang et al. [64], in the work of Gao et al., negatively charged inert spheres were collected near the TiO₂ side. To maintain symmetry, when one SiO₂ sphere was adsorbed, the dimer was of a snowman structure. When two or more SiO₂ particles were adsorbed, the tracer spheres were uniformly distributed at the same symmetry line on the TiO₂ side. When the symmetry line was completely occupied by SiO₂, the latter tracers were attached to the former tracers' gap position. After the UV lamp was turned off, the photocatalytic reaction-H⁺ concentration gradient dissipated, and the tracers detached from the motor surface.

Sen et al. studied the aggregation and dispersion of self-diffusiophoretic AgCl motors and SiO₂ similarly to the case of TiO₂. Under UV and visible light irradiation, the motors released H⁺ and Cl⁻, forming a local electric field directed to the interior, where the motors repelled each other under electrophoresis. When the UV light was turned off, the local electric field formed by ion diffusion disappeared, and the motors gathered again. It was presumed that the Ag produced under UV light changed the motor's surface properties and made it sensitive to visible light [70].

The above examples show how motors can direct the “assembly” and “dissolution” of inert spheres, while Palacci et al. used motors to

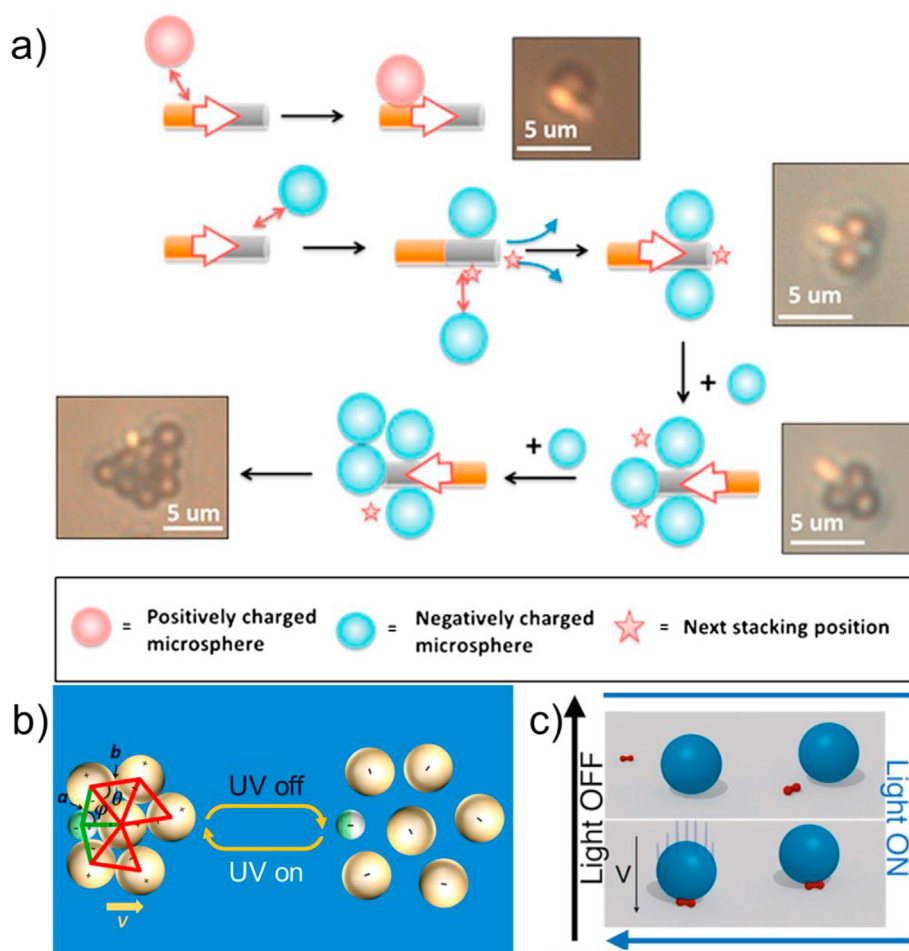


Fig. 5. Chemical communication between motors and tracer particles. a) Positively charged, inert microspheres migrate toward Au/Pt micromotors via electrophoresis and eventually attach to their surfaces [64]. b) When switching UV on and off, reversible assembly of TiO₂ (green) and SiO₂ (yellow) clusters occurs by self-electrophoresis [68]. c) Upon switching blue light on and off, and steered by a magnetic field, a hematite particle can transport and release a cargo (passive sphere) via diffusiophoresis [69].

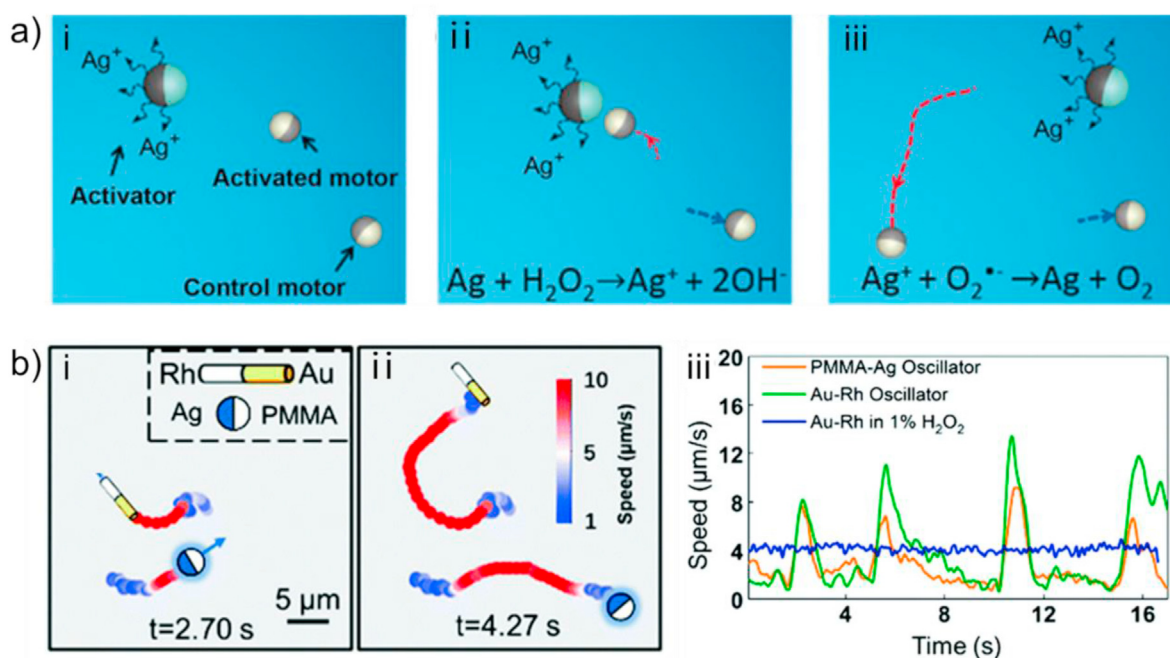


Fig. 6. One-way chemical communication between motors of two types. a) A (PS)/Ni/Au/Ag motor releases Ag⁺ ions in the H₂O₂ solution. Ag⁺ ions are then reduced to metallic Ag and deposit on the surface of the SiO₂/Pt motor, enhancing the catalytic activity of the SiO₂/Pt motor for H₂O₂ decomposition, and increasing its speed [71]. b) Non-oscillating motors start to oscillate under the action of Ag⁺ released from oscillating motors [72].

transport inert objects as shown in Fig. 5c [69]. Under blue light irradiation, peanut-shaped hematite motors ($\sim 1.5 \mu\text{m}$ long and $\sim 0.6 \mu\text{m}$ wide) catalyzed the decomposition of hydrogen peroxide, resulting in a local concentration gradient, which moves motors along their short axis by diffusiophoresis. Under the action of the electric field, the positively charged fluid near the substrate moved in the direction of motors, thereby loading up 1–20 μm cargo. These motors were also weakly magnetic, so a magnetic field can guide motors to find cargos, transport them to the designated location, and then release them by turning off the light.

3.2. One-way signal communication between two motors

In a unidirectional communication exchange between two motors, one motor acts as a generator and emits a signal in response to an external stimulus, while the other motor responds to the corresponding command and does not send a signal in return. In contrast to Section 3.1, in the following examples the object receiving the chemical signal is itself capable of moving autonomously. Upon receiving the signal, it can change its speed or even mode of motion. Unidirectional communication between two motors enriches the information transfer compared to inert spheres, and the motor receiving the information can also perform more complex tasks.

Unidirectional chemical communication between motors can increase the speed of the signal-receiving motor. Both (PS)/Ni/Au/Ag and SiO_2/Pt motors moved by self-diffusiophoresis powered by the catalytic decomposition of H_2O_2 [71]. As shown in Fig. 6a below, (PS)/Ni/Au/Ag motors produced Ag^+ during the catalytic decomposition process, which was then deposited on the Pt end of the SiO_2/Pt motor. Under the effect of O_2^- , the presence of Ag sites on the Pt surface separates the catalytic sites on the Pt, thus increasing the H_2O_2 catalytic decomposition rate and accelerating the SiO_2/Pt motors' speed.

Zhou et al. designed motors with the ability to “learn” and change their motion after receiving information from other motors (Fig. 6b) [72]. Under UV illumination and a mixed solution of H_2O_2 and KCl, Ag-PMMA motors underwent a redox reaction on their surfaces to achieve a cyclic transition between Ag and AgCl, which resulted in a periodic oscillatory motion. The authors mixed the oscillating Ag-PMMA spheres with Pt-PS spheres and Au-Rh rod motors, which do not have the oscillating ability. After that, the Pt-PS and Au-Rh also oscillated by “learning” from an oscillating motor. This was due to the release of Ag^+ from the oscillating Ag-PMMA motor during redox reactions, which led to the anisotropic deposition of Ag^+ on the surface of a Pt-PS or Au-Rh motor by diffusion and reduction, in a way similar to an early study from Chen et al. [71].

Even in studies that were not explicitly designed to foster communication between motors, motors can release chemical signals. This can provide a choice for the subsequent design of motor communication. For example, Gao et al. prepared a motor with a spherical head of Ag and a rod-shaped SiO_2 tail, which moved with silver in front in H_2O_2 [73]. The authors argue that the motor catalyzes the decomposition of H_2O_2 to produce Ag^+ and HOO^- , which could act as a messenger to communicate with other objects. As discussed in section 2.1.2 in the context of micromotors' response to chemical gradients, Archer et al. designed and fabricated Janus motors from the pH-responsive hydrogel poly(2-vinyl pyridine) (PVP) with a Pt cap that exhibited a controlled release of chemicals in response to changes in pH [30]. In response to pH decreases, the PVP swells to release the loaded chemicals. Therefore, this type of motor can also become a choice as a chemical messenger or could be used in applications where the release of payload in acidic pH is desired (such as drug delivery near a tumor, where the pH is acidic compared to normal tissue). Notably, pH-induced swelling also causes the speed to decrease because of the increased drag profile. Thus, the motors tend to accumulate and release their cargo simultaneously in the most acidic regions, where drugs are most needed.

3.3. Mutual interaction between two signal-releasing motors

We now consider interactions between two different motors that can each act as both senders and receivers of chemical signals. This type of interaction, which is more complex than the previous two, results in intriguing phenomena such as oligomers, reversible clusters, specific patterns, predator-prey, and leader-follower behaviors. Understanding how motors communicate with each other can help us better design motors for efficient communication and cope with complex application scenarios. Here, we will discuss communication between motors of the same kind and those of different kinds. Although clustering could arguably be considered a form of motor-motor communication, here we consider clustering to be a *consequence* of motor-motor communication, since this review is focused on *chemical* communication between micromotors and their surroundings.

In addition to communication between Au/Pt rods and inert particles, the above-mentioned study by Wang et al. also investigated the intercommunication of self-electrophoretic Au–Pt rods, which could assemble into stable interlocking dimers and trimers (Fig. 7a) [64]. In an H_2O_2 solution, the Au side underwent a reduction reaction to consume H^+ , while the Pt side underwent an oxidation reaction to produce H^+ , forming a local electric field. As mentioned above, this led to dipolar charge clouds surrounding each individual motor, with the fluid surrounding Pt and Au carrying a positive and negative charge, respectively. When two motors came close to each other, electrostatic attraction was generated, and rods arranged into staggered dimers as well as trimers. The Pt and Au surfaces of adjacent rods tended to attract one another (i.e., there was negligible Pt/Pt or Au/Au attraction). Mou et al. also studied the formation of dimers, trimers, and tetramers by TiO_2/Pt motors, which moved and assembled by the same mechanism as the example above (Fig. 7b) [74].

The above two examples are based on interactions among a relatively small number of motors, but in practice, dozens of motors (or more) will be required to perform complicated tasks, such as drug delivery or water remediation. Deng et al. achieved the generation and disintegration of TiO_2/Pt motor clusters by cycling UV light on and off [16]. When the UV was turned off, the TiO_2/Pt motor formed clusters because of the spontaneous dissociation of the functional groups on the TiO_2 surface [75]; when the UV was turned on, the photochemical reaction produced repulsive phoretic interactions, the motors repelled each other and the clusters disintegrated.

In the above experiments, the dynamics of aggregation and repulsion are observed only if the external conditions change. In contrast, Theurkauff et al. demonstrated that Au/Pt motors spontaneously formed dynamic clusters even if the external conditions were not changed, and clusters were continually disintegrating as motors joined and left clusters [76]. In 2013, a similar phenomenon of active crystals formed by hematite particles was found by Palacci et al. [77]. Under blue light, the hematite catalyzed decomposition of hydrogen peroxide, generating a concentration gradient, which led to diffusiophoresis and osmosis effects that led to formation of “living crystals.” When the light was turned off, microspheres scattered. When the light was turned on, the particles aggregated under the effect of phoresis, osmosis and steric resistance. Since the osmosis of clusters themselves was in the same direction as the phoresis on individual particles, the phoresis-driven attraction further caused the particles to assemble into compact crystals.

A large amount of work has investigated the phenomenon of dynamic cluster formation, but it is unclear whether its lifetime is random or dependent on specific parameters. Ginot et al. analyzed the fusion and separation rates of a large number of Au–Pt Janus micromotor clusters in relation to size and derived a dependence of cluster lifetime and size, providing a comprehensive description of the dynamics of dynamic clusters [78].

In addition to assembling crystals by mutual exchange of motors, motors can also be designed to assemble in specific patterns. Zhou et al. designed a “HIT” pattern based on the mutual interaction of Fe_2O_3

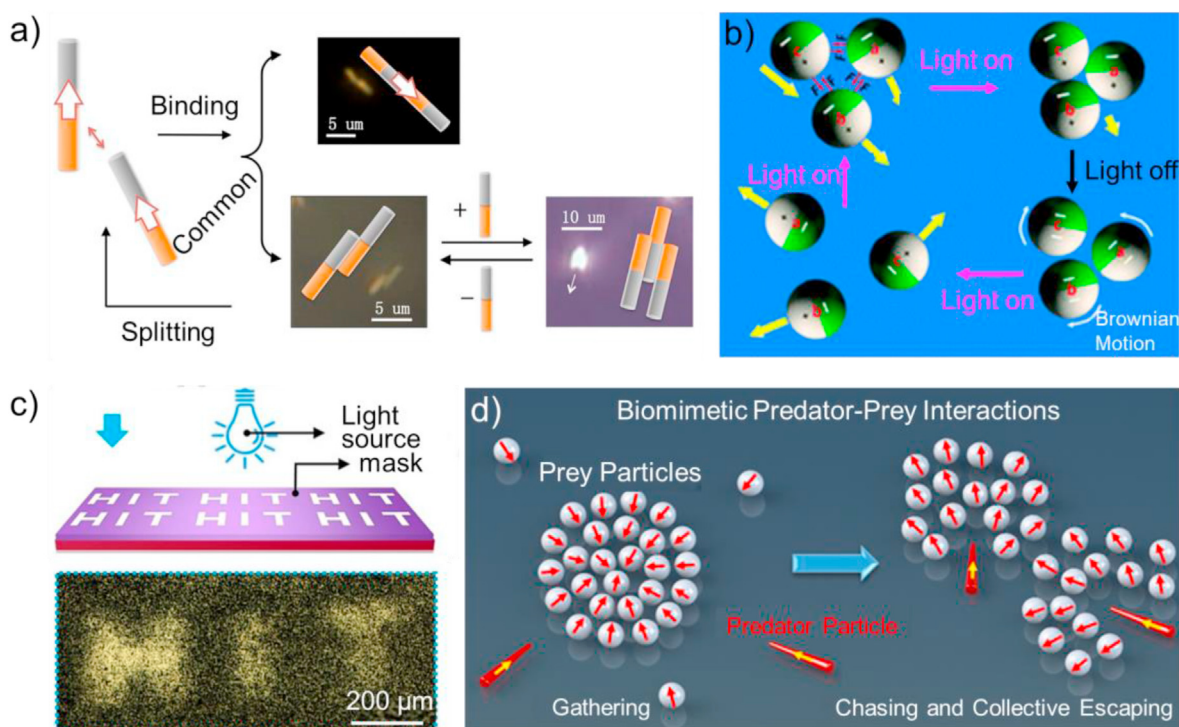


Fig. 7. Mutual interaction between two signal-releasing motors. a) Au–Pt rods self-assemble into dimers and trimers of staggered shapes [64]. b) TiO₂/Pt Janus motors aggregate or disperse upon switching light [74]. c) Self-assembled HIT pattern of Fe₂O₃ nanomotors induced by light [79]. d) Schematic of biomimetic predator–prey interactions between micromotors of two species [80].

motors [79]. The mask and actual pattern assembled by the motors are shown in Fig. 7c. In an aqueous H₂O₂ solution, pure Fe₂O₃ microspheres produce Fe³⁺ and OH⁻ when illuminated by UV light. Due to the different diffusion rates of the two ions, a local electric field pointing away from the motor was generated, which repelled the positively

charged Fe₂O₃ neighbors, and drove an electroosmotic flow along the substrate in the same direction. Therefore, the authors effectively observed negative-phototaxis, accumulation of motors in the dark region.

As our knowledge of and control over the interactions among micromotors has continued to improve, it is now possible to design a

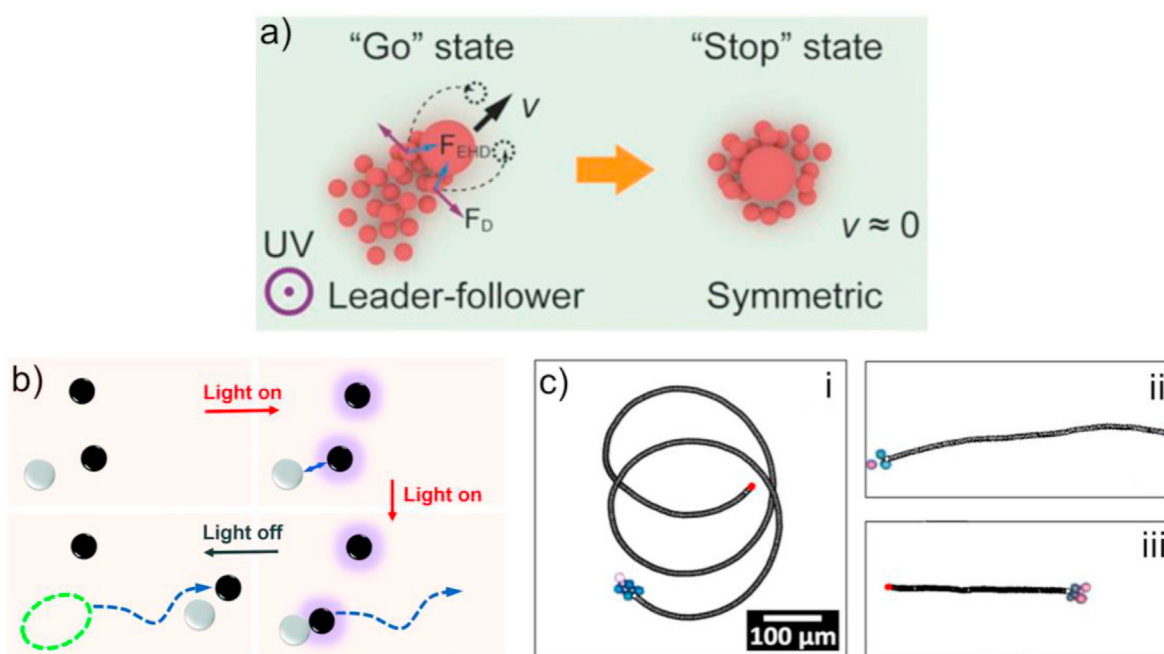


Fig. 8. Interaction among non-motile particles generates directional motion. a) TiO₂ microspheres assemble leader-follower-like structure and move taking advantage of the converging electrohydrodynamic flows under an electric field. When UV is on, the repulsive diffusiophoretic force reverts the assembly to a more symmetric configuration and thus stops the assembly [81]. b) Non-motile TiO₂ and SiO₂ particles assemble into a dimer with directional movement [82]. c) Clusters formed by positive and negative ion exchange resin particles can move in straight or rotating trajectories [83].

system where micromotors communicate across species. For example, Mou et al. studied mutual communication between two different motors, with similar predator-prey relationships to those seen in nature (Fig. 7d) [80]. In this experiment, TiO₂ microspheres and ZnO microrods were mixed together, both of which are asymmetric microparticles (arising from synthesis imperfections) that spontaneously move under light, likely via ionic self-diffusiophoresis. A local electric field was formed pointing towards the TiO₂, and the electroosmotic flow near the substrate also drove the surrounding TiO₂ to spontaneously aggregate. Conversely, the local electric field near the ZnO microrods and the electroosmotic flow was in the opposite direction, so ZnO microrods spontaneously repelled each other. When ZnO microrods move close to a TiO₂ population, their respective chemical and electric fields overlap, and the TiO₂ population escaped from the ZnO microrods similar to a how a prey escapes from its predator.

In some cases, non-motile colloidal particles of two different types do not function as motors on their own but produce directional motion when in proximity to one another. Although strictly speaking these particles are not micromotors, they can provide inspiration for the design of future modes of communication among motors.

For example, Liang et al. showed that TiO₂ particles of different sizes can assemble and produce directional movement (Fig. 8a) [81]. By controlling the UV and electric field, the assembly could stop and move reversibly. In their experiment, a convergent electrohydrodynamic (EHD) flow was generated around the dielectric micro/nanoparticles under an AC electric field. The convergent EHD flow of larger particles is stronger, which induced surrounding particles of different sizes to form a cluster. The anisotropic EHD flow around the cluster caused it to move. As the cluster moved forward, it can further grow by absorbing more microparticles through the EHD force. The larger particles in the cluster tended to act as leaders in the forward movement, followed by several smaller particles. When the UV was turned on, O₂ molecules were generated around TiO₂, so under the chemiosmotic slip, the particles were propelled away from each other. At the same time, the strong EHD flow around the large TiO₂ attracted the small TiO₂. In the end, the small TiO₂ was symmetrically distributed around the large TiO₂, so the EHD of the team was symmetrical and the whole team will stop until the UV is turned off.

The signal producing particle TiO₂ can also release chemicals to attract inert SiO₂ spheres, thereby assembling into dimers and generating motion. In the experiments of Yu et al., under UV irradiation, H₂O₂ was photocatalytically decomposed on the surface of TiO₂ spheres and generated chemical gradients [82]. As shown in Fig. 8b, the inert SiO₂ spheres gradually approached the TiO₂ and combined into dimers, breaking the symmetry of isotropic TiO₂ spheres.

Two active spheres with opposite chemical fields will attract each other and move in a linear or circular motion depending on the number of active spheres attracted [83]. Fig. 8c shows the different movements of clusters. A cationic exchange particle (IEX) is a resin that exchanges the cations in the environment with H⁺. Due to the difference in the diffusion speed of the cations being exchanged, both the generated local electric field and the electroosmotic flow near the substrate pointed to the cationic IEX. Yet, the local electric field and the electroosmotic flow induced by an anionic IEX, one that replaces anions with OH⁻, was opposite and relatively weaker, so the electroosmotic flow between them pointed to the cationic IEX. When the opposite IEXs approached, they would assemble into multimers. The flows resulting from the anion IEX push the cation IEX forward and block the anion IEX until they both travel at the same speed.

More recently, Meredith et al. demonstrated “predator-prey” interaction between the two oil droplets immersed in water [84]. Two mutually miscible oil droplets, 1-bromooctane (BOct) and ethoxynonafluorobutane (EFB), are dispersed in the water phase. When a BOct droplet is close enough to a EFB droplet, the EFB droplet can dissolve small BOct droplets that are solubilized around a large BOct droplet, releasing solubilizers and decreasing the interfacial tension of the side of

the BOct droplet near the EFB droplet, so the BOct approached the EFB droplet like a predator approaching its prey. In a similar spirit (but very different construction), the Tang lab recently reported how ZnO nanorods could chemically couple to ion exchange microspheres [85], where the “waste” products of the ion exchange particles (protons to be specific) are the “nutrient” of the ZnO rods, while the Zn²⁺ ions released by the latter attract and provide for the ion exchange particles as well. This two-way feedback leads to enhanced activity of both species and even active swarms. These two examples represent the recent progress in designing self-propelled micromotors with biomimicking interactions.

4. Conclusion

The practical application of micro-nanomotors requires communication between motors and their environment, and between themselves, both of which require a motor to respond to local environmental changes. In this paper, we have reviewed recent experimental progress related to chemical release and communication among micromotors. In section 2, we introduced three types of local chemical release methods: (i) spontaneous diffusion of preloaded chemicals, (ii) the release of reactants in response to external stimuli, and (iii) controlled release of preloaded chemicals via “gate control.” These strategies of altering motors’ local chemical microenvironment form the backbone of designing motors that communicate. Section 3 then introduced micromotor communication at three levels: (i) micromotor communication with inert objects, by which inert objects can be aggregated, repelled, and transported by the motor; (ii) unidirectional communication between micromotors, in which the motor receiving the signal can be accelerated and acquire the ability to “learn”; (iii) bidirectional communication between the same or different micromotors, which can lead to the formation of reversible active clusters, patterning, and biomimetic behaviors. Throughout the article, we have shown numerous examples where, in response to an external stimulus, motors release chemical signals to exchange information with their surroundings and the other motors, a critical function for targeted therapy, biosensing, and environmental monitoring.

We also acknowledge that some highly complex real-world environments may stymie some micromotor designs, and thus be too hostile for coordinated, collective behavior mediated by communication between motors. For example, although the Pt/Au motors have been widely studied and show many fascinating behaviors, their reliance on hydrogen peroxide fuel and poor performance in electrically conductive media (as is the case with some other microswimmer designs as well) may prevent some of these behaviors from being realized beyond the laboratory. As another example, if the micromotors are immersed in a strong shear flow, the hydrodynamic forces imposed by that flow may overwhelm the tendency of the swimmers to cluster, undergo chemotaxis, or some other communication-mediated behavior. Thus, basic research efforts should continue toward developing robust micromotors capable of operating in complex, even hostile environments.

Going forward, it will be important to develop novel micromotor fabrication strategies that show tendency to exhibit chemotaxis in steady-state chemical gradients. Chemotaxis-mediated communication between motile cells is important for a variety of biological processes, such as the functioning of the mammalian immune system. Tumors are widely known to exhibit gradients in pH, temperature, oxygen concentration, and pressure; artificial micromotors that exhibit true chemotaxis are thus promising for payload delivery in these environments. To achieve this, micromotors loaded with enzymes are a promising target [86,87]. When suspended in solution of their substrate, many enzymes generate enough mechanical force as a byproduct of their normal catalytic activity to propel themselves, and there is increasing evidence that they exhibit chemotaxis as well [47,48,88–90].

Several research frontiers are worthy of future exploration. In most previous studies, a singular chemical message is typically released, which means that motors receiving this message are poised to perform a single task. It would be interesting to consider a system where multiple

chemical signals are transmitted, and where motors can select which signal to send or receive, or exhibit signal-processing capabilities. Second, most of the responses described in this article are based on the principles of electrokinetics, i.e., electrophoresis, diffusiophoresis and associated osmotic flows along surfaces. Although these effects are useful and powerful, it is important to expand our toolbox by including additional interaction mechanisms. For example, we can imagine a motor that releases special chemicals and changes the surface state (surface activity, reaction) of another motor [72,84], which then changes its dynamics by stops/starts, accelerating or decelerating. Preliminary studies in this direction have been reported (see ref. 72 for an example), but more efforts are clearly needed. Finally, the level of complexity is rather primitive in the studies we have reviewed here, while in actual applications, a micromotor might be asked to sense the signal changes in the external environment and acts as a messenger to pass on the detected information to the others, and communicates between its peers, which then cooperate and get the job done. Preliminary studies of oscillating micromotors that show synchronization and propagating waves are promising in this front [91–93], but there still remains many scientific and technological challenges before this biomimetic principle can be translated to a coordinated micro-robot swarm.

As more scientists from diverse disciplines enter the field, the march will continue toward an idealized micromotor system that includes in-depth communication between motors with different functions, exchange of complex information, mobility of a large group of motors, and a distributed workload. We sincerely hope that this review article assists in achieving this goal.

Declaration of competing interest

The authors declare that they have no known competing financial interests or personal relationships that could have appeared to influence the work reported in this paper.

Acknowledgement

LH and WW are grateful for the financial support from the National Science Foundation of Guangdong Province (No. 2017B030306005), the National Natural Science Foundation of China (11774075), and the Science Technology and Innovation Program of Shenzhen (JCYJ20190806144807401). JLM gratefully acknowledges support from start-up funds at George Mason University.

References

- [1] R.D. Vale, R.A. Milligan, The way things move: looking under the hood of molecular motor proteins, *Science* 288 (2000) 88–95.
- [2] P.H. Colberg, S.Y. Reigh, B. Robertson, R. Kapral, Chemistry in motion: tiny synthetic motors, *Acc. Chem. Res.* 47 (2014) 3504–3511.
- [3] J. Shao, M. Xuan, T. Si, L. Dai, Q. He, Biointerfacing polymeric microcapsules for in vivo near-infrared light-triggered drug release, *Nanoscale* 7 (2015) 19092–19098.
- [4] Z. Wu, T. Si, W. Gao, X. Lin, J. Wang, Q. He, Superfast near-infrared light-driven polymer multilayer rockets, *Small* 12 (2016) 577–582.
- [5] W. Wang, S. Li, L. Mair, S. Ahmed, T.J. Huang, T.E. Mallouk, Acoustic propulsion of nanorod motors inside living cells, *Angew. Chem. Int. Ed.* 53 (2014) 3201–3204.
- [6] C. Zhou, L. Zhao, M. Wei, W. Wang, Twists and turns of orbiting and spinning metallic microparticles powered by megahertz ultrasound, *ACS Nano* 11 (2017) 12668–12676.
- [7] L. Baraban, R. Streubel, D. Makarov, L. Han, D. Karnausenko, O.G. Schmidt, G. Cuniberti, Fuel-free locomotion of Janus motors: magnetically induced thermophoresis, *ACS Nano* 7 (2013) 1360–1367.
- [8] L. Soler, S. Sánchez, Catalytic nanomotors for environmental monitoring and water remediation, *Nanoscale* 6 (2014) 7175–7182.
- [9] J. Orozco, V. García-Gradiña, M. D'Agostino, W. Gao, A. Cortés, J. Wang, Artificial enzyme-powered microfish for water-quality testing, *ACS Nano* 7 (2013) 818–824.
- [10] D. Xu, Y. Wang, C. Liang, Y. You, S. Sanchez, X. Ma, Self-propelled micro/nanomotors for on-demand biomedical cargo transportation, *Small* 16 (2020) 1902464.
- [11] Y. Wu, X. Lin, Z. Wu, H. Möhwald, Q. He, Self-propelled polymer multilayer Janus capsules for effective drug delivery and light-triggered release, *ACS Appl. Mater. Interfaces* 6 (2014) 10476–10481.

- [12] W. Wang, T.-Y. Chiang, D. Velegol, T.E. Mallouk, Understanding the efficiency of autonomous nano- and microscale motors, *J. Am. Chem. Soc.* 135 (2013) 10557–10565.
- [13] S. Balasubramanian, D. Kagan, C.-M. JackHu, S. Campuzano, M.J. Lobo-Castañón, N. Lim, D.Y. Kang, M. Zimmerman, L. Zhang, J. Wang, Micromachine-Enabled capture and isolation of cancer cells in complex media, *Angew. Chem. Int. Ed.* 50 (2011) 4161–4164.
- [14] H. Wang, M. Pumera, Coordinated behaviors of artificial micro/nanomachines: from mutual interactions to interactions with the environment, *Chem. Soc. Rev.* 49 (2020) 3211–3230.
- [15] W. Wang, L.A. Castro, M. Hoyos, T.E. Mallouk, Autonomous motion of metallic microrods propelled by ultrasound, *ACS Nano* 6 (2012) 6122–6132.
- [16] Z. Deng, F. Mou, S. Tang, L. Xu, M. Luo, J. Guan, Swarming and collective migration of micromotors under near infrared light, *Appl. Mater. Today* 13 (2018) 45–53.
- [17] J. Yan, M. Han, J. Zhang, C. Xu, E. Luijten, S. Granick, Reconfiguring active particles by electrostatic imbalance, *Nat. Mater.* 15 (2016) 1095–1099.
- [18] G. Zhao, H. Wang, S. Sanchez, O.G. Schmidt, M. Pumera, Artificial micro-cinderella based on self-propelled micromagnets for the active separation of paramagnetic particles, *Chem. Commun.* 49 (2013) 5147–5149.
- [19] R. Boch, D. Shearer, B. Stone, Identification of iso-amyl acetate as an active component in the sting pheromone of the honey bee, *Nature* 195 (1962) 1018–1020.
- [20] W. Han, Y. Lou, J. Tang, Y. Zhang, Y. Chen, Y. Li, W. Gu, J. Huang, L. Gui, Y. Tang, F. Li, Q. Song, C. Di, L. Wang, Q. Shi, R. Sun, D. Xia, M. Rui, J. Tang, D. Ma, Molecular cloning and characterization of chemokine-like factor 1 (CKLF1), a novel human cytokine with unique structure and potential chemotactic activity, *Biochem. J.* 357 (2001) 127–135.
- [21] J. Adler, Chemotaxis in *Escherichia coli*, in: *Behaviour of Micro-organisms*, Springer, 1973, pp. 1–15.
- [22] P.K. Ghosh, Y. Li, F. Marchesoni, F. Nori, Pseudochemotactic drifts of artificial microwimmers, *Phys. Rev.* 92 (2015), 012114.
- [23] C. Chen, X. Chang, P. Angsantikul, J. Li, B. Esteban-Fernández de Ávila, E. Karshalev, W. Liu, F. Mou, S. He, R. Castillo, Y. Liang, J. Guan, L. Zhang, J. Wang, Chemotactic guidance of synthetic organic/inorganic payloads functionalized sperm micromotors, *Adv. Biosyst.* 2 (2018) 1700160.
- [24] J. Shao, M. Xuan, H. Zhang, X. Lin, Z. Wu, Q. He, Chemotaxis-guided hybrid neutrophil micromotors for targeted drug transport, *Angew. Chem. Int. Ed.* 56 (2017) 12935–12939.
- [25] P.C. Wilkinson, J.M. Lackie, J.V. Forrester, G.A. Dunn, Chemokinetic accumulation of human neutrophils on immune complex-coated substrata: analysis at a boundary, *J. Cell Biol.* 99 (1984) 1761–1768.
- [26] Y. Hong, N.M.K. Blackman, N.D. Kopp, A. Sen, D. Velegol, Chemotaxis of nonbiological colloidal rods, *Phys. Rev. Lett.* 99 (2007) 178103.
- [27] J.L. Moran, P.M. Wheat, N.A. Marine, J.D. Posner, Chemokinesis-driven accumulation of active colloids in low-mobility regions of fuel gradients, *Sci. Rep.* 11 (2021) 4785.
- [28] T. Bhuyan, A.K. Singh, D. Dutta, A. Unal, S.S. Ghosh, D. Bandyopadhyay, Magnetic field guided chemotaxis of iMushbots for targeted anticancer therapeutics, *ACS Biomater. Sci. Eng.* 3 (2017) 1627–1640.
- [29] K.K. Dey, S. Bhandari, D. Bandyopadhyay, S. Basu, A. Chattopadhyay, The pH taxis of an intelligent catalytic microbot, *Small* 9 (2013) 1916–1920.
- [30] R.A. Archer, J.R. Howse, S. Fujii, H. Kawashima, G.A. Buxton, S.J. Ebbens, pH-responsive catalytic Janus motors with autonomous navigation and cargo-release functions, *Adv. Funct. Mater.* 30 (2020) 2000324.
- [31] Y. Kato, S. Ozawa, C. Miyamoto, Y. Maehata, A. Suzuki, T. Maeda, Y. Baba, Acidic extracellular microenvironment and cancer, *Canc. Cell Int.* 13 (2013) 89.
- [32] I. Lagzi, S. Soh, P.J. Wesson, K.P. Browne, B.A. Grzybowski, Maze solving by chemotactic droplets, *J. Am. Chem. Soc.* 132 (2010) 1198–1199.
- [33] A. Banerjee, I. Williams, R.N. Azevedo, M.E. Helgeson, T.M. Squires, Solutio-inertial phenomena: designing long-range, long-lasting, surface-specific interactions in suspensions, *Proc. Natl. Acad. Sci. U.S.A.* 113 (2016) 8612–8617.
- [34] C. Jin, C. Krüger, C.C. Maass, Chemotaxis and autochemotaxis of self-propelling droplet swimmers, *Proc. Natl. Acad. Sci. Unit. States Am.* 114 (2017) 5089.
- [35] J. Adler, Chemotaxis in bacteria, *Annu. Rev. Biochem.* 44 (1975) 341–356.
- [36] D.C. Prieve, J.L. Anderson, J.P. Ebel, M.E. Lowell, Motion of a particle generated by chemical gradients. Part 2. Electrolytes, *J. Fluid Mech.* 148 (1984) 247.
- [37] H.J. Keh, Diffusiophoresis, in: D. Li (Ed.), *Encyclopedia of Microfluidics and Nanofluidics*, Springer US, Boston, MA, 2008, pp. 365–369.
- [38] S. Zeng, C.-H. Chen, J.C. Mikkelsen, J.G. Santiago, Fabrication and characterization of electroosmotic micropumps, *Sensor. Actuator. B Chem.* 79 (2001) 107–114.
- [39] D. Wu, Signaling mechanisms for regulation of chemotaxis, *Cell Res.* 15 (2005) 52–56.
- [40] P.C. Wilkinson, Assays of leukocyte locomotion and chemotaxis, *J. Immunol. Methods* 216 (1998) 139–153.
- [41] M.R. D'Orsogna, M.A. Suchard, T. Chou, Interplay of chemotaxis and chemokinesis mechanisms in bacterial dynamics, *Phys. Rev.* 68 (2003), 021925.
- [42] D. Ralt, M. Manor, A. Cohen-Dayag, I. Tur-Kaspa, I. Ben-Shlomo, A. Makler, I. Yuli, J. Dor, S. Blumberg, S. Mashiah, et al., Chemotaxis and chemokinesis of human spermatozoa to follicular factors, *Biol. Reprod.* 50 (1994) 774–785.
- [43] S.H. Zigmond, J.G. Hirsch, Leukocyte locomotion and chemotaxis. New methods for evaluation, and demonstration of a cell-derived chemotactic factor, *J. Exp. Med.* 137 (1973) 387–410.
- [44] Dunn, G. A., Chemotaxis as a form of directed cell behaviour: some theoretical considerations. *Biol. Chemot. Resp.* 1981, 1–26.
- [45] M.N. Popescu, W.E. Uspal, C. Bechinger, P. Fischer, Chemotaxis of active Janus nanoparticles, *Nano Lett.* 18 (2018) 5345–5349.

- [46] R. Golestanian, T.B. Liverpool, A. Ajdari, Designing phoretic micro- and nano-swimmers, *New J. Phys.* 9 (2007) 126–126.
- [47] A. Somasundar, S. Ghosh, F. Mohajerani, L.N. Massenbarg, T. Yang, P.S. Cremer, D. Velegol, A. Sen, Positive and negative chemotaxis of enzyme-coated liposome motors, *Nat. Nanotechnol.* 14 (2019) 1129–1134.
- [48] A. Joseph, C. Contini, D. Cecchin, S. Nyberg, L. Ruiz-Perez, J. Gaitzsch, G. Fullstone, X. Tian, J. Azizi, J. Preston, G. Volpe, G. Battaglia, Chemotactic synthetic vesicles: design and applications in blood-brain barrier crossing, *Sci. Adv.* 3 (2017), e1700362.
- [49] H. Zhang, K. Yeung, J.S. Robbins, R.A. Pavlick, M. Wu, R. Liu, A. Sen, S.T. Phillips, Self-powered microscale pumps based on analyte-initiated depolymerization reactions, *Angew. Chem. Int. Ed.* 51 (2012) 2400–2404.
- [50] M.S. Baker, V. Yadav, A. Sen, S.T. Phillips, A self-powered polymeric material that responds autonomously and continuously to fleeting stimuli, *Angew. Chem. Int. Ed.* 52 (2013) 10295–10299.
- [51] V. Yadav, H. Zhang, R. Pavlick, A. Sen, Triggered “on/off” micropumps and colloidal photodiode, *J. Am. Chem. Soc.* 134 (2012) 15688–15691.
- [52] Y. Hong, M. Diaz, U.M. Córdova-Figueroa, A. Sen, Light-driven titanium-dioxide-based reversible microfireworks and micromotor/micropump systems, *Adv. Funct. Mater.* 20 (2010) 1568–1576.
- [53] R. Dong, Q. Zhang, W. Gao, A. Pei, B. Ren, Highly efficient light-driven TiO₂-Au Janus micromotors, *ACS Nano* 10 (2016) 839–844.
- [54] A. Banerjee, T.M. Squires, Long-range, selective, on-demand suspension interactions: combining and triggering soluto-inertial beacons, *Sci. Adv.* 5 (2019) eaax1893.
- [55] Y.-Z. You, K.K. Kalebaila, S.L. Brock, D. Oupický, Temperature-controlled uptake and release in PNIPAM-modified porous silica nanoparticles, *Chem. Mater.* 20 (2008) 3354–3359.
- [56] Y. Ji, X. Lin, H. Zhang, Y. Wu, J. Li, Q. He, Thermoresponsive polymer brush modulation on the direction of motion of phoretically driven Janus micromotors, *Angew. Chem. Int. Ed.* 58 (2019) 4184–4188.
- [57] H. Wan, Y. Zhang, Z. Liu, G. Xu, G. Huang, Y. Ji, Z. Xiong, Q. Zhang, J. Dong, W. Zhang, H. Zou, Facile fabrication of a near-infrared responsive nanocarrier for spatiotemporally controlled chemo-photothermal synergistic cancer therapy, *Nanoscale* 6 (2014) 8743–8753.
- [58] S. Dühr, D. Braun, Why molecules move along a temperature gradient, *Proc. Natl. Acad. Sci. Unit. States Am.* 103 (2006) 19678–19682.
- [59] Y. Wen, L. Xu, W. Wang, D. Wang, H. Du, X. Zhang, Highly efficient remote controlled release system based on light-driven DNA nanomachine functionalized mesoporous silica, *Nanoscale* 4 (2012) 4473–4476.
- [60] C. Wang, Z. Li, D. Cao, Y.-L. Zhao, J.W. Gaines, O.A. Bozdemir, M.W. Ambrogio, M. Frasconi, Y.Y. Botros, J.I. Zink, J.F. Stoddart, Stimulated release of size-selected cargos in succession from mesoporous silica nanoparticles, *Angew. Chem. Int. Ed.* 51 (2012) 5460–5465.
- [61] P. Díez, E. Lucena-Sánchez, A. Escudero, A. Llopis-Lorente, R. Villalonga, R. Martínez-Máñez, Ultrafast directional Janus Pt-mesoporous silica nanomotors for smart drug delivery, *ACS Nano* 15 (3) (2021) 4467–4480.
- [62] Q. Zhao, H. Geng, Y. Wang, Y. Gao, J. Huang, Y. Wang, J. Zhang, S. Wang, Hyaluronic acid oligosaccharide modified redox-responsive mesoporous silica nanoparticles for targeted drug delivery, *ACS Appl. Mater. Interfaces* 6 (2014) 20290–20299.
- [63] D. Kagan, P. Calvo-Marzal, S. Balasubramanian, S. Sattayasamitsathit, K.M. Manesh, G.-U. Flechsig, J. Wang, Chemical sensing based on catalytic nanomotors: motion-based detection of trace silver, *J. Am. Chem. Soc.* 131 (2009) 12082–12083.
- [64] W. Wang, W. Duan, A. Sen, T.E. Mallouk, Catalytically powered dynamic assembly of rod-shaped nanomotors and passive tracer particles, *Proc. Natl. Acad. Sci. U.S.A.* 110 (2013) 17744–17749.
- [65] W.F. Paxton, A. Sen, T.E. Mallouk, Motility of catalytic nanoparticles through self-generated forces, *Chemistry* 11 (2005) 6462–6470.
- [66] J.L. Moran, P.M. Wheat, J.D. Posner, Locomotion of electrocatalytic nanomotors due to reaction induced charge autoelectrophoresis, *Phys. Rev.* 81 (2010), 065302.
- [67] J.L. Moran, J.D. Posner, Electrokinetic locomotion due to reaction-induced charge auto-electrophoresis, *J. Fluid Mech.* 680 (2011) 31–66.
- [68] Y. Gao, F. Mou, Y. Feng, S. Che, W. Li, L. Xu, J. Guan, Dynamic colloidal molecules maneuvered by light-controlled Janus micromotors, *ACS Appl. Mater. Interfaces* 9 (2017) 22704–22712.
- [69] J. Palacci, S. Sacanna, A. Vatchinsky, P.M. Chaikin, D.J. Pine, Photoactivated colloidal dockers for cargo transportation, *J. Am. Chem. Soc.* 135 (2013) 15978–15981.
- [70] M.E. Ibele, P.E. Lammert, V.H. Crespi, A. Sen, Emergent, collective oscillations of self-mobile particles and patterned surfaces under redox conditions, *ACS Nano* 4 (2010) 4845–4851.
- [71] C. Chen, X. Chang, H. Teymourian, D.E. Ramírez-Herrera, B. Esteban-FernándezdeÁvila, X. Lu, J. Li, S. He, C. Fang, Y. Liang, F. Mou, J. Guan, J. Wang, Bioinspired chemical communication between synthetic nanomotors, *Angew. Chem. Int. Ed.* 57 (2018) 241–245.
- [72] C. Zhou, Q. Wang, X. Lv, W. Wang, Non-oscillatory micromotors “learn” to oscillate on-the-fly from oscillating Ag micromotors, *Chem. Commun.* 56 (2020) 6499–6502.
- [73] Y. Gao, R.P. Dullens, D.G. Aarts, Bulk synthesis of silver-head colloidal rodlike micromotors, *Soft Matter* 14 (2018) 7119–7125.
- [74] F. Mou, L. Kong, C. Chen, Z. Chen, L. Xu, J. Guan, Light-controlled propulsion, aggregation and separation of water-fuelled TiO₂/Pt Janus submicromotors and their “on-the-fly” photocatalytic activities, *Nanoscale* 8 (2016) 4976–4983.
- [75] F. Mou, J. Zhang, Z. Wu, S. Du, Z. Zhang, L. Xu, J. Guan, Phototactic flocking of photochemical micromotors, *iScience* 19 (2019) 415–424.
- [76] I. Theurkauff, C. Cottin-Bizonne, J. Palacci, C. Ybert, L. Bocquet, Dynamic clustering in active colloidal suspensions with chemical signaling, *Phys. Rev. Lett.* 108 (2012) 268303.
- [77] J. Palacci, S. Sacanna, A.P. Steinberg, D.J. Pine, P.M. Chaikin, Living crystals of light-activated colloidal surfers, *Science* 339 (2013) 936–940.
- [78] F. Ginot, I. Theurkauff, F. Detcheverry, C. Ybert, C. Cottin-Bizonne, Aggregation-fragmentation and individual dynamics of active clusters, *Nat. Commun.* 9 (2018) 696.
- [79] D. Zhou, Y. Gao, H. Liu, G. Zhang, L. Li, Light-induced patterned self-assembly behavior of isotropic semiconductor nanomotors, *Chem. Asian J.* 14 (2019) 2445–2449.
- [80] F. Mou, X. Li, Q. Xie, J. Zhang, K. Xiong, L. Xu, J. Guan, Active micromotor systems built from passive particles with biomimetic predator–prey interactions, *ACS Nano* 14 (2020) 406–414.
- [81] X. Liang, F. Mou, Z. Huang, J. Zhang, M. You, L. Xu, M. Luo, J. Guan, Hierarchical microswarms with leader–follower-like structures: electrohydrodynamic self-organization and multimode collective photoresponses, *Adv. Funct. Mater.* 30 (2020) 1908602.
- [82] T. Yu, P. Chuphal, S. Thakur, S.Y. Reigh, D.P. Singh, P. Fischer, Chemical micromotors self-assemble and self-propel by spontaneous symmetry breaking, *Chem. Commun.* 54 (2018) 11933–11936.
- [83] R. Niu, A. Fischer, T. Palberg, T. Speck, Dynamics of binary active clusters driven by ion-exchange particles, *ACS Nano* 12 (2018) 10932–10938.
- [84] C.H. Meredith, P.G. Moerman, J. Groenewold, Y.-J. Chiu, W.K. Kegel, A. van Blaaderen, L.D. Zarzar, Predator–prey interactions between droplets driven by non-reciprocal oil exchange, *Nat. Chem.* 12 (2020) 1136–1142.
- [85] C. Wu, J. Dai, X. Li, L. Gao, J. Wang, J. Liu, J. Zheng, X. Zhan, J. Chen, X. Cheng, M. Yang, J. Tang, Ion-exchange enabled synthetic swarm, *Nat. Nanotechnol.* 16 (3) (2021), <https://doi.org/10.1038/s41565-020-00825-9>.
- [86] X. Zhao, K. Gentile, F. Mohajerani, A. Sen, Powering motion with enzymes, *Acc. Chem. Res.* 51 (2018) 2373–2381.
- [87] S. Ghosh, A. Somasundar, A. Sen, Enzymes as active matter, *Ann. Rev. Condens. Matter Phys.* 12 (2021) null.
- [88] F. Peng, Y. Tu, J.C.M. van Hest, D.A. Wilson, Self-guided supramolecular cargo-loaded nanomotors with chemotactic behavior towards cells, *Angew. Chem. Int. Ed. Engl.* 54 (2015) 11662–11665.
- [89] W.-S. Jang, H.J. Kim, C. Gao, D. Lee, D.A. Hammer, Enzymatically powered surface-associated self-motile protocells, *Small* 14 (2018) 1801715.
- [90] S. Ghosh, A. Somasundar, A. Sen, Enzymes as active matter, *Ann. Rev. Condens. Matter Phys.* 12 (2021) 177–200.
- [91] A. Altemose, M.A. Sánchez-Farrán, W. Duan, S. Schulz, A. Borhan, V.H. Crespi, A. Sen, Chemically controlled spatiotemporal oscillations of colloidal assemblies, *Angew. Chem. Int. Ed.* 56 (2017) 7817–7821.
- [92] C. Zhou, N.J. Suenamatsu, Y. Peng, Q. Wang, X. Chen, Y. Gao, W. Wang, Coordinating an ensemble of chemical micromotors via spontaneous synchronization, *ACS Nano* 14 (2020) 5360–5370.
- [93] C. Zhou, X. Chen, Z. Han, W. Wang, Photochemically excited, pulsating Janus colloidal motors of tunable dynamics, *ACS Nano* 13 (2019) 4064–4072.